Hindawi
Modelling and Simulation in Engineering
Volume 2023, Article ID 5728385, 17 pages
https://doi.org/10.1155/2023/5728385

Research Article

Two-Dimensional FEM Approach of Metabolic Effect on Thermoregulation in Human Dermal Parts During Walking and Marathon

Dev Chandra Shrestha, Saraswati Acharya, and Dil Bahadur Gurung

Department of Mathematics, School of Science, Kathmandu University, Dhulikhel, Nepal

Correspondence should be addressed to Saraswati Acharya; saraswati.acharya@ku.edu.np

Received 29 April 2022; Revised 19 May 2023; Accepted 6 June 2023; Published 27 June 2023

Academic Editor: Angelos Markopoulos

The physiological mechanisms conduction, convection, and radiation exchange the heat energy in bi-directional routes between the body and the temperature field. Metabolism and evaporation are the uni-directional routes for the exchange of heat energy. In the metabolic process, the body creates internal heat energy, whereas the body loses excess heat energy through the evaporation process and maintains the body temperature. This study has shown steady and unsteady state temperature distribution in three skin layers: epidermis, dermis, and subcutaneous tissue, during walking and marathon. The results have analyzed that each skin layer temperature is higher during a marathon compared with walking due to more metabolic effects. The computation has been carried out for the two-dimensional Pennes' bio-heat equation using a finite element approach. The generated results have been exhibited graphically.

1. Thermal Regulation Mechanism

Human organisms maintain or control heat energy, primarily through the radiation, convection, metabolism, diffusion, and evaporation processes. Radiation, diffusion, and convection contribute to receiving heat energy when the ambient temperature is higher than skin temperature and losing heat energy when the ambient temperature is lower than skin temperature. Hypothalamus is the central unit and plays a significant role in thermoregulatory responses. It checks the current body's core temperature and compares it with the natural temperature of about 37°C. If the body's core temperature is too low, the body generates and maintains heat through the processes of shivering or metabolism to sustain a healthy life. If the current body core temperature is too high, the surplus heat is eliminated by the evaporation process, which cools the skin and maintains the body temperature. Metabolic heat generation, thermal environmental heat load, and heat loss capacity are the key components of the heat balance equation.

During walking, the body creates metabolic heat energy and dissipates it on the body's surface. There is no storage heat energy. As a result, the body is thermally balanced. The heat gain and heat loss by the body is in equilibrium. Therefore, the heat exchange between the body and the temperature field is minimum, and the body core temperature maintains constant at 37°C. Since the body core temperature is proportional to the metabolic rate and largely independent of a wide range of environmental conditions. In a temperate or cool environment, the body loses heat energy through the convection process and reduces the skin's blood flow rate. The physiological mechanisms are only incapable to maintain the body temperature. Therefore, additional clothing or external heating, require to better the body temperature in a cold climate. Marathon racers suffer more heat stress than walkers [1]. Furthermore, the fast movement of muscle mass during the marathon releases a large amount of metabolic heat energy, which cannot be dissipated instantly. Therefore, the rate of heat loss is not equivalent to the heat gain rate. The storage of metabolic heat energy causes skin temperature to rise. It also increases the body core temperature up to 39.5°C [2]. If the body mechanism is unable to control the body core temperature higher than 39.5°C, the temperature

causes cell death [3]. Sweat evaporation is the primary factor to maintain the body temperature in a hot environment. The sweat vaporization from the skin depends on the surface area exposed to the surroundings, convective airflow around the body, ambient temperature, and relative humidity of ambient air. In a hot environment, during walking, the average sweating rate is 170.83 ml/hour [4]. During the marathon in a hot environment, the skin and the body core temperature increase due to rapid skin blood flow. At the same time, due to the body mechanism, the eccrine sweat glands become active and lose the excess heat energy in the form of sweat vapor from the body [5]. The body loses sweat upto 10 liters per day by occurring the sensible perspiration process and controls the body temperature, preventing the body from hyperthermia disorder [4]. This shows that sweat loss affects significantly by the activity level.

The evaporate rate is independent of the temperature gradient between the skin and the environment. On the other hand, sweat rate is proportional to the water vapor pressure gradient between the skin and the environment.

Convection is the heat exchange process between the fluid and the body. The heat exchange rate depends on the direction and the speed of the fluid flow. The convective heat exchange rate increases by increasing the temperature gradient between the fluid flow and the skin surface. A healthy body loses about 15% of heat energy through this process [6].

Radiation is the electromagnetic heat transfer mechanism from the sun to the body without contact with the surface. This radiation penetrates through to the earth's surface, increases the body's temperature, and loses heat energy through infrared radiation. If the body temperature is higher than the ambient temperature, more heat emits than is received. The body loses about 60% of heat energy by the radiation process at rest in a temperate room [6]. The sun rays of a wavelength longer than 3×10^{-6} m absorb by the atmospheric environment and do not reach the earth's surface due to having a less penetrating force. On the other hand, the radiation of a wavelength shorter than 4×10^{-6} m does not affect the skin surface [7]. Thus, the skin's capability to reflect the light of a shorter wavelength assists the possibilities of their radiating almost perfectly. The driving force of radiation heat loss depends on a large temperature gradient between the body and environment temperatures. The radiated heat energy by the skin surface given by Stefan's Boltzmann as;

$$E_r = \sigma\varepsilon\left(T^4 - {T_\infty}^4\right), \tag{1}$$

where E_r is the radiative heat energy, σ is the Stefan Boltzmann constant, ε is the emissivity of the skin surface depending on the emitter of wavelength and Plank constant, T is the absolute temperature of the skin surface, and T_∞ is the temperature of the temperature field.

Conduction is another process that occurs in the human body to exchange heat from or to the body directly in contact with other objects. If the body is warmer, then it loses heat. If the body is colder, it gains heat from the contact objects. The heat flow rate is the same in each direction if the body is in the thermal equilibrium position [8].

$$E_s = E_m - W_w - E_e \pm E_r \pm E_{co} \pm E_{cv}, \tag{2}$$

where E_s is the storage heat energy, E_m is the metabolic heat energy, W_w is the work energy, E_e is the evaporative heat energy, E_r is the radiative heat energy, E_{co} is the conductive heat energy, and E_{cv} is the convective heat energy.

Skin blood flow plays a crucial role in maintaining body temperature, whereas the blood flow rate significantly changes in the presence of a magnetic field [9]. The blood flow rate reflects by the temperature gradient between the body core temperature and the skin surface temperature [10]. The hypothalamus regulates skin blood flow and changes the skin temperature. In a cold environment, the skin blood flow decreases by the vasoconstriction process due to narrow blood vessels. It minimizes the loss of heat energy from the body. In a hot environment, the skin blood flow rate rises through the vasodilation process due to expanding the blood vessel. The continuous increase in blood flow controls by maintaining the pressure with the help of active muscle.

The parameter thermal conductivity also affects the tissue temperature. It has various values at different temperatures. The temperature of the tissue, which is above the healthy range, decreases as the thermal conductivity of the blood decreases [11].

Basal metabolic rate (BMR) is the minimum energy required for a person to sustain a healthy life at rest. The BMR depends upon the body weight [12]. In the metabolic process, the fat adipose tissue rapidly breaks down to produce a large amount of heat energy and maintains the body's core temperature. During walking, the muscles are the primary source of metabolic heat. In the marathon, the inhaled oxygen rate of the body and exhaled carbon dioxide rate from the body also increase. These help in increasing the metabolism to provide the necessary energy.

During walking and marathon, most of the organs come in movement. Therefore, the body requires additional energy that substitutes by the metabolic process. The metabolic rate increases as much as 15 times above the resting level in the marathon [13]. In this process, the body loses the thermal energy generated by the organs. On increasing the metabolic rate, half of the increased metabolic energy uses to maintain the skin temperature and evaporates heat energy from the body in the form of a tear. The remaining metabolic energy is used to increase the blood flow rate and body core temperature. The continuous blood flow controls by the body mechanism by rapidly increasing the metabolic rate at the beginning of exercises and becomes constant after a certain period. Therefore, the metabolic rate $S(t)$ has logistic behavior given by equation (3) [14].

$$S(t) = \left(S_0 + \frac{E - S_0}{1 + e^{-\beta(t-t_0)}}\right), \tag{3}$$

where S_0 is the BMR (w/m^3), t is activity time (seconds), E is the activities threshold metabolism (w/m^3), β is an activity controlled parameter (/seconds), and t_0 (seconds) is the Sigmoid's midpoint of the curve over time t for extensive exercise. The basal metabolism is the minimum required metabolic energy to sustain life at rest. The threshold metabolism is the upper limit of the metabolic value, and the Sigmoid midpoint is the middle of the period, from where the phenomena of the curve change.

The average BMR in a healthy adult human body is 1114 w/m^3, but it may vary from person to person. The unsteady to steady behavior of metabolic rate for walking is 3889.43 w/m^3 and during a marathon is 7918 w/m^3 [14, 15]. The behavior of metabolic rate during the marathon and walking is graphically shown in Figure 1.

Blood perfusion is the nutritious delivery process of arterial blood to a capillary bed in the biological tissue. Changes in blood perfusion may be more complicated to detect in skin layers. A decrease in blood perfusion below normal levels is associated with ill health, and raising skin blood perfusion above normal levels has a beneficial or detrimental effect on different organs of the body [16]. Change in blood perfusion rate has an enhancing effect on thermoregulation in the human body [17]. The difference between the blood perfusion rates in the artery to the vein is negligible. In capillary, the rate of blood flow is slow, so takes place the equilibrium position.

First, the perfusion has been formulated by Pennes' and proposed a mathematical model equation incorporated into the standard thermal diffusion and metabolism given by [18].

$$\rho c \frac{\partial T}{\partial t} = \nabla \cdot (K \nabla T) + \rho_b c_b w_b (T_A - T) + S(t), \quad (4)$$

equation (4) is known as Pennes' bio-heat equation.

Pennes' analyzed the effect of thermal diffusivity, perfusion, and metabolism components in living tissue and calculated the temperature of the human forearm. He checked the validity of the temperature results obtained by his predicated equation with experimentally measured temperature in the human forearm.

By using equation (3), Pennes' equation is modified to;

$$\rho c \frac{\partial T}{\partial t} = \nabla \cdot (K \nabla T) + \rho_b c_b w_b (T_A - T) + \left(S_0 + \frac{E - S_0}{1 + e^{-\beta(t - t_0)}} \right), \quad (5)$$

where c_b is the blood-specific heat capacity (J/kg°C), ρ_b is the blood density (kg/m^3), w_b is blood perfusion rate (kg/m^3 s), ρ is the tissue density (kg/m^3), c is the tissue-specific heat capacity (J/kg°C), K is the tissue thermal conductivity (J/ms°C), T_A is the arterial blood temperature (°C), and T is the tissue temperature (°C).

Exercises, such as walking and marathon, are beneficial for health. They play a remarkable role to keeps the body healthy. However, some novelty problem arises due to the long marathon. Training and racing for marathons can also cause muscle damage due to repetitive muscle contractions. During the marathon, kidney cells become damaged by the lack of blood flow to the organs and the loss of fluid volume but typically recover within two days. For those who are participating in a long marathon, and intake insufficient oxygen, it seems the risk of sudden cardiac death is approximately 2.5 times greater than during walking [19].

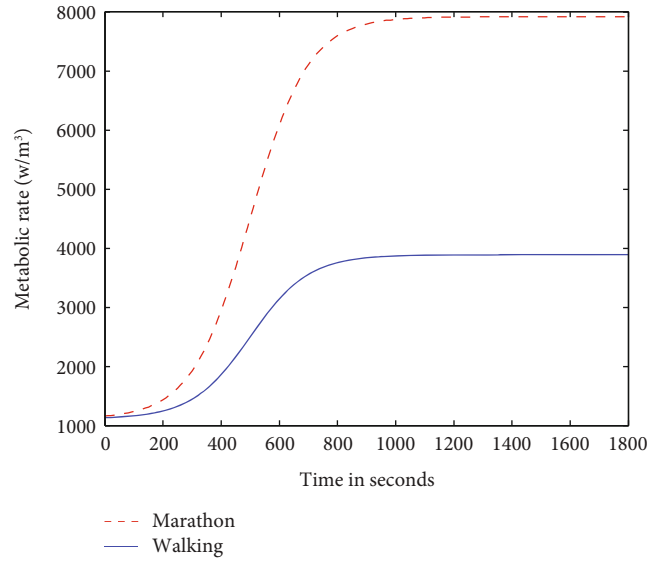

Figure 1: Metabolic rate behavior during marathon and walking.

Gokul et al. [20] studied the effect of blood perfusion and metabolism on temperature distribution in the human eye. They suggested that eye temperature is negligibly affected by blood perfusion and metabolism, but is affected by the parameters of blood temperature, ambient temperature, and evaporation rate. Acharya et al. [21] compared the metabolic effect in thermoregulation on the human male and female skin layers in a two-dimensional finite element method. The study deals that males lead to higher skin temperature than females due to thinner skin layers in males. Agrawal et al. [22] prepared a model for the temperature distribution in a human limb by assuming an irregular tapered shape limb with a variable radius and eccentricity. Gurung [23] prepared a model in two-dimensional temperature distribution in the human dermal region exposed at low ambient temperature with airflow. Kenefick et al. [2] experimentally studied the temperature of skin layers during the marathon and noticed that the maximum body core temperature reaches 39.5°C. This temperature is proportional to the metabolic rate and largely independent of the environmental condition during the exercise period. Khanday and Sexana [24] observed the thermoregulation and fluid regulation in the human head and dermal parts at cold ambient conditions by using the finite element method.

Previous researchers prepared models that have presented the temperature distribution in the human dermal parts with various sweating rates and ambient temperatures with constant metabolic rates. However, this model is prepared for the temperature distribution in the dermal part of the human body using the different metabolic rates

produced during walking and marathon. The excess heat energy loses and keeps the body in thermoregulation by the body mechanism, which provides the realistic temperature of the dermal parts. The finite element approach has been used for numerical results and graphs of the temperature profiles.

2. Methods

In two-dimensional discretization of the dermal layers, the skin thickness 'L' has been taken along Y-axis, and the width of the skin 'W' has been taken along the X-axis on the skin surface. The outer surface of the body has exposed to the environment, so heat loss occurs by convection, radiation, and sweat evaporation. The mixed boundary condition of heat flux from the outer skin surface is given by [21]:

$$\Gamma_1 : -K\frac{\partial T}{\partial y}\bigg|_{y=0} = h_{\mathrm{cv}}(T - T_\infty) + \sigma\varepsilon\left({T_\infty}^4 - T^4\right) + LE, \quad (6)$$

where h_{cv} is the convective heat transfer coefficient between the skin and the temperature field ($\mathrm{w/m^2\,^\circ C}$), T_∞ is the atmospheric temperature ($^\circ$C), σ is the Stefan Boltzmann constant ($5.67 \times 10^{-8}\,\mathrm{w/m^2\,^\circ C}$), ε is the emissivity of the skin surface, L is the latent heat of evaporation (J/kg), and E is the evaporative heat loss between the skin surface and the temperature field ($\mathrm{kg/m^2\,s}$).

The radiation term presented in equation (6) is nonlinear. Therefore, it is difficult to find the solution of equation (6). For the solution of the problem, we introduce a suitable iterative method. The above nonlinear boundary condition stated in equation (6) can be written as;

$$\Gamma_1 : -K\frac{\partial T_1}{\partial y}\bigg|_{y=0} = \left[h_{cv} + \sigma\varepsilon\left(T_1 + {T_\infty}^2\right)(T_1 + T_\infty)\right](T_1 - T_\infty) + LE. \quad (7)$$

If the value of the term $[(T_1 + {T_\infty}^2)(T_1 + T_\infty)]$ is known, equation (6) can be viewed as a generalized convection condition between convection and radiation. For this, we introduce the iterative algorithm:

$$\Gamma_1 : -K\frac{\partial T_1^{(N)}}{\partial y}\bigg|_{y=0} = h_{\mathrm{cr}}\left(T_1^{(N)} - T_\infty\right) + LE, \quad (8)$$

with

$$h_{\mathrm{cr}} = h_{\mathrm{cv}} + \sigma\varepsilon\left(T_1^{(N-1)} + T_\infty\right)\left(T_1^{(N-1)2} + {T_\infty}^2\right), \quad (9)$$

where h_{cr} is the combined heat transfer coefficient of convection and radiation with radiation coefficient $\sigma\varepsilon(T_1^{(N-1)} + T_\infty)(T_1^{(N-1)2} + {T_\infty}^2)$.

The term $T_1^{(N)}$ is the temperature sequences for $N = 1, 2, 3, \ldots,$ and $T_1^{(0)}$ is the initial guess temperature of the skin surface. The iteration process has completed when the convergent condition is satisfied.

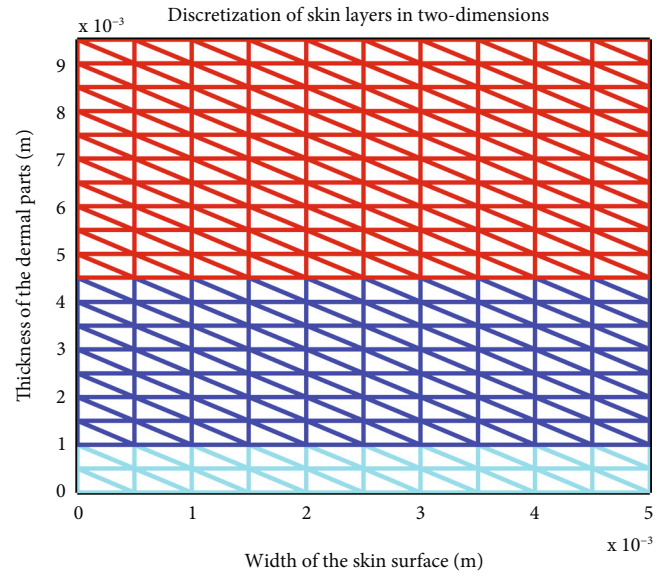

Figure 2: Discretization of skin thickness in 380 meshes.

$$\left\| T_1^{(N)} - T_1^{(N-1)} \right\| < \delta, \quad (10)$$

where $\delta > 0$ is the specified interaction tolerance.

The transport of heat within tissue occurs along normal to the skin surface from the body core, and hence we assume negligible heat flux in the x-direction. Therefore, the boundary conditions are assumed to be:

$$\Gamma_2 : \frac{\partial T}{\partial x}\bigg|_{x=0} = 0, \quad (11)$$

$$\Gamma_3 : \frac{\partial T}{\partial x}\bigg|_{x=W} = 0. \quad (12)$$

During marathon and walking, the human body maintains its body core temperature uniformly by 39.5°C and 37°C, respectively. Therefore, the inner boundary condition has taken as:

$$\begin{aligned} \Gamma_4 &: T(x, L) = T_{\mathrm{b}} = 37^\circ\mathrm{C} \quad \text{during walking,} \\ \Gamma_5 &: T(x, L) = T_{\mathrm{b}} = 39.5^\circ\mathrm{C} \quad \text{during marathon.} \end{aligned}, \quad (13)$$

Γ_4 and Γ_5 are the Dirichlet's boundary conditions during walking and marathon, respectively, and T_{b} is the body core temperature.

3. Skin Geometry and Assumption Parameters

3.1. Skin Geometry. Skin plays a protective role and performs various functions in the thermoregulatory process. The skin thickness in the human body has divided into three primary layers: epidermis, dermis, and subcutaneous tissue. Each skin layer has its own thermo-physical and optical properties [25].

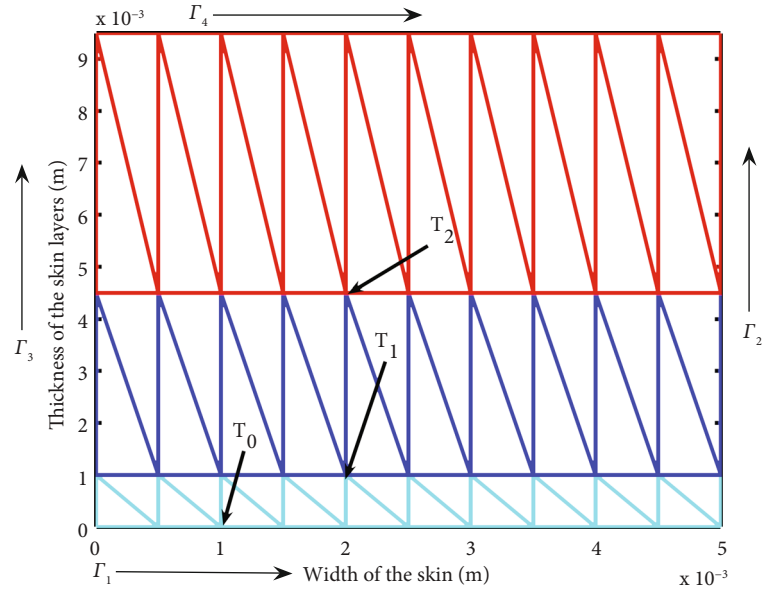

FIGURE 3: Discretization of skin thickness into the epidermis, dermis, and subcutaneous tissue.

The outer layer epidermis provides mechanical strength and rigidity to the skin's structure. The epidermis contains melanocytes that produce melanin pigments. Melanin helps to change the skin's color and protect the body from ultraviolet radiation when the sunlight incident on the skin's surface. The middle layer dermis contains blood vessels, elastic fibers, and collagen. The primary role of the dermis is to support the epidermis and enable the skin to thrive. It is responsible for the contraction or dilation of the blood vessels to maintain homeostasis body. During walking and marathon in a hot environment, the blood volume increases due to dilating the blood vessel and releasing the heat in the form of sweat.

The subcutaneous tissue is the inner layer of tissue, which has composed of adipose fat cells. It works as insulation to maintain our body's core temperature and prevent hyperthermia sickness when the body exposes to a hot environment. In the model, the skin thickness has considered as a two-dimensional rectangular skin region. The skin diameter (width) along the X-axis is 5×10^{-3} m, and the total thickness along the vertical Y-axis is 9.5×10^{-3} m. Initially, the skin is divided into 380 elements with a triangular shape and has 220 nodes. The epidermis layer, dermis layer, and subcutaneous tissue have divided into 40, 140, and 200 triangular meshes and have 33, 88, and 121 nodes, respectively, as shown in Figure 2. Figure 3 depicts the discretization of skin thickness into the epidermis, dermis, and subcutaneous tissue with their respective nodal temperatures, T_0, T_1, and T_2.

A triangular element 'e' has three global Cartesian coordinates: $A(x_1, y_1)$, $B(x_2, y_2)$, and $C(x_3, y_3)$ has taken as shown in Figure 4. Each node temperature has expressed in the form of shape (interpolation) functions [26]. We assume that the temperature field (trial function) over the element 'e' is given by

$$T^e(x, y) = a_0 + a_1 x + a_2 y. \tag{14}$$

On reducing the nodal temperature at the nodal point 1, 2, and 3, we get:

$$\begin{aligned} T_1^e(x, y) &= a_0 + a_1 x_1 + a_2 y_1 \\ T_2^e(x, y) &= a_0 + a_1 x_2 + a_2 y_2 \\ T_3^e(x, y) &= a_0 + a_1 x_3 + a_2 y_3 \end{aligned} \tag{15}$$

On solving equation (15) we get,

$$\begin{bmatrix} a_0 \\ a_1 \\ a_2 \end{bmatrix} = \begin{bmatrix} 1 & x_1 & y_1 \\ 1 & x_2 & y_2 \\ 1 & x_3 & y_3 \end{bmatrix}^{-1} \begin{bmatrix} T_1^e \\ T_2^e \\ T_3^e \end{bmatrix}. \tag{16}$$

Let us assume, $\begin{vmatrix} 1 & x_1 & y_1 \\ 1 & x_2 & y_2 \\ 1 & x_3 & y_3 \end{vmatrix} = 2 \times$ area of triangular element $= 2\Delta$ and

$$\begin{aligned} x_2 y_3 - x_3 y_2 &= \alpha_1, \quad y_2 - y_3 = \beta_1, \quad x_3 - x_2 = \gamma_1 \\ x_3 y_1 - x_1 y_3 &= \alpha_2, \quad y_3 - y_1 = \beta_2, \quad x_1 - x_3 = \gamma_2 \\ x_1 y_2 - x_2 y_1 &= \alpha_3, \quad y_1 - y_2 = \beta_3, \quad x_2 - x_1 = \gamma_3 \end{aligned} \tag{17}$$

Then equation (13) becomes as,

$$\begin{bmatrix} a_0 \\ a_1 \\ a_2 \end{bmatrix} = \begin{bmatrix} \alpha_1 & \alpha_2 & \alpha_3 \\ \beta_1 & \beta_2 & \beta_2 \\ \gamma_1 & \gamma_2 & \gamma_3 \end{bmatrix} \begin{bmatrix} T_1^e \\ T_2^e \\ T_3^e \end{bmatrix}. \tag{18}$$

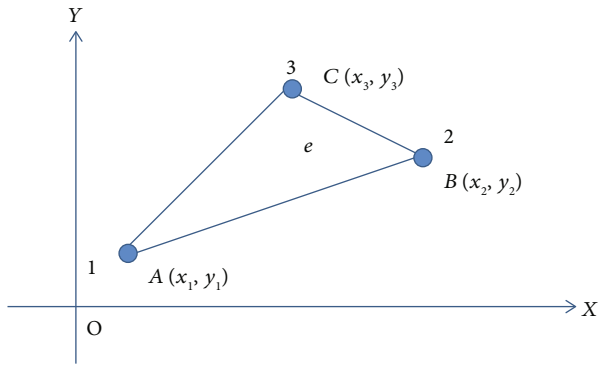

Figure 4: Triangular element with three nodes.

Table 1: The thickness of skin layers used in the model [27].

Skin layers	Epidermis layer (L_1)m	Dermis layer $(L_2 - L_1)$m	Subcutaneous layer $(L_3 - L_2)$m
Thickness (m)	0.001	0.0035	0.005

This provides, $a_0 = \alpha_1 T_1^{(e)} + \alpha_2 T_2^{(e)} + \alpha_3 T_3^{(e)}/2\Delta$, $a_1 = \beta_1 T_1^{(e)} + \beta_2 T_2^{(e)} + \beta_3 T_3^{(e)}/2\Delta$, and $a_2 = \gamma_1 T_1^{(e)} + \gamma_2 T_2^{(e)} + \gamma_3 T_3^{(e)}/2\Delta$.

Using a_0, a_1, and a_2 in equation (14), finally we get,

$$T^e(x,y) = \left(\frac{\alpha_1 + \beta_1 x + \gamma_1 y}{2\Delta}\right) T_1^e + \left(\frac{\alpha_2 + \beta_2 x + \gamma_2 y}{2\Delta}\right) T_2^e + \left(\frac{\alpha_3 + \beta_3 x + \gamma_3 y}{2\Delta}\right) T_3^e,$$
$$T^e(x,y) = N_1 T_1^e + N_2 T_2^e + N_3 T_3^e \tag{19}$$

where N_i, $(i = 1, 2, 3)$ is a shape function written as, $\alpha_i + \beta_i x + \gamma_i y/2\Delta = N_i$, $\forall i = 1, 2, 3$.

3.2. Assumption Parameters. Since the epidermis layer is composed of the dead cell, therefore, the arterial blood temperature T_A, blood perfusion rate (ρ_b), and metabolic heat generation rate $(S(t))$ have been taken to zero in the epidermis layer [21]. The arterial blood temperature T_A in the dermis and subcutaneous tissue are assumed equal to T_b. During walking and marathon races, the adipose tissue becomes more active and increases metabolic energy. Therefore, the metabolic rate $(S(t))$ in the subcutaneous tissue is taken double that of the dermis layer. Since the blood perfusion rate has been considered a function of depth, however in this model, the perfusion rate is considered as same in the dermis and subcutaneous region.

4. Solution of the Model

The governing equation (5) together with boundary conditions is transformed into the variational form:

$$I = \frac{1}{2}\iint_\Omega \left[K\left(\left(\frac{\partial T}{\partial x}\right)^2 + \left(\frac{\partial T}{\partial y}\right)^2\right) + \rho_b c_b w_b (T_A - T)^2 - 2\left(S_0 + \frac{E - S_0}{1 + e^{-\beta(t-t_0)}}\right) T\right] d\Omega + \frac{1}{2}\iint_\Omega \left[\rho c \frac{\partial T^2}{\partial t}\right] d\Omega + \frac{1}{2}\int_{\Gamma_1^{(e)}} \left[h_{cr}(T - T_\infty)^2 + LET\right] d\Gamma_1 \tag{20}$$

where Ω is the domain of the region of the dermal parts and Γ_1 is the outer boundary of the skin. On expressing the function I as the sum of E elemental quantities $T^{(e)}$ as

$$I = \sum_{e=1}^{E} I^{(e)}, \tag{21}$$

where

$$I^{(e)} = \frac{1}{2}\int\int_{\Omega^{(e)}} \left[K^{(e)}\left(\left(\frac{\partial T^{(e)}}{\partial x}\right)^2 + \left(\frac{\partial T^{(e)}}{\partial y}\right)^2\right) + \rho_b c_b w_b^{(e)} \left(T_A - T^{(e)}\right)^2\right] d\Omega^{(e)} - \left[2\left(S_0 + \frac{E - S_0}{1 + e^{-\beta(t-t_0)}}\right)^{(e)} T^{(e)} - \rho c \frac{\partial T^{2(e)}}{\partial t}\right] d\Omega^{(e)} + \frac{1}{2}\int_{\Gamma_1^{(e)}} \left[h_{cr}\left(T^{(e)} - T_\infty\right)^2 + LET^e\right] d\Gamma_1^{(e)} \tag{22}$$

Here, $\Omega^{(e)}$ is the domain of the element 'e'. Equation (22) is broken into six parts as below.

$$I^{(e)} = I_1^{(e)} + I_2^{(e)} - I_3^{(e)} + I_4^{(e)} + I_5^{(e)} + I_6^{(e)}, \tag{23}$$

Table 2: Parameter values used in the model [14, 27].

Parameter	L	K_1	K_2	K_3	h_{cr}	$M_2 = M_3$	$\rho_1 = \rho_2 = \rho_3$	$c_1 = c_2 = c_3$
Value	2.42×10^6	0.209	0.314	0.418	6.27	1254	1050	3475
Unit	J/kg	w/m ˚C	w/m ˚C	w/m ˚C	w/m^2 ˚C	w/m^3 ˚C	kg/m^3	J/kg ˚C

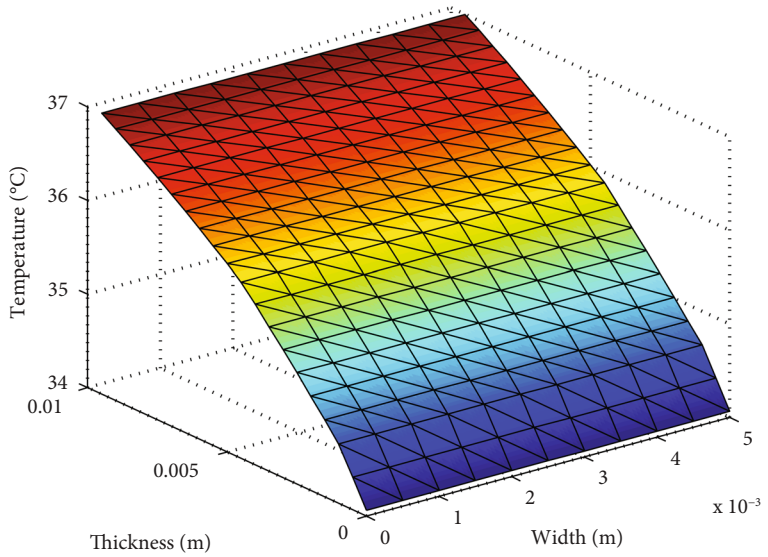

(a)

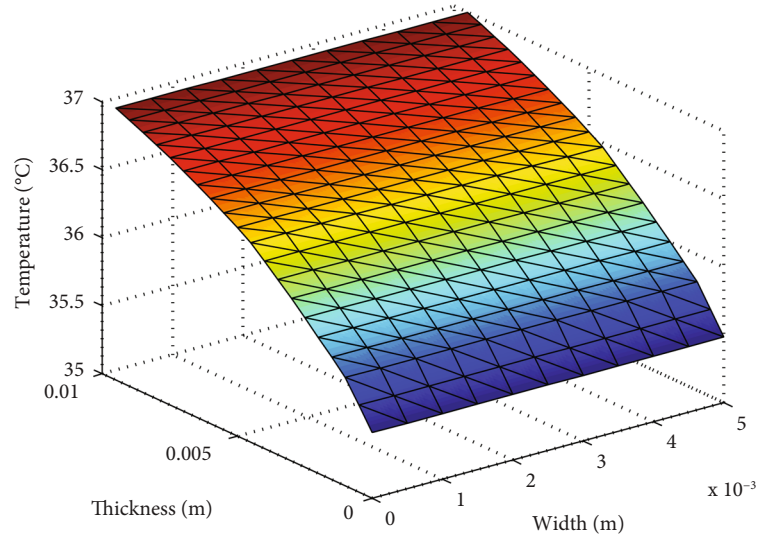

(b)

Figure 5: Continued.

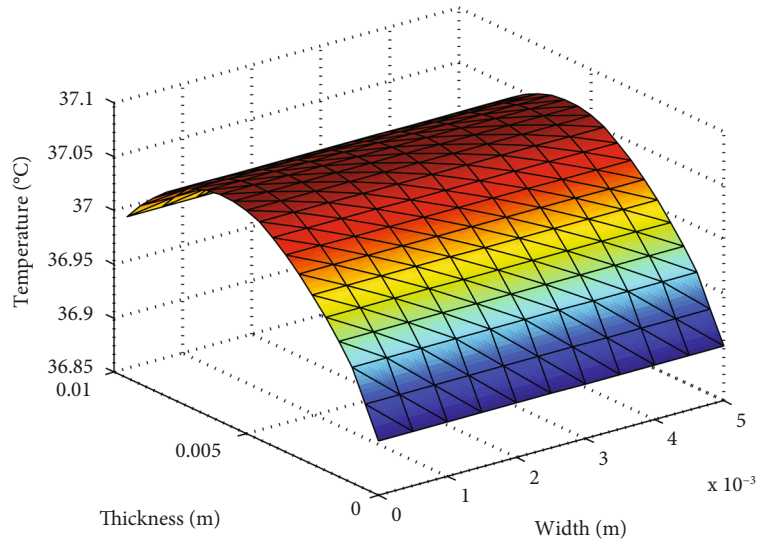

(c)

FIGURE 5: Estimation of steady state temperatures of the epidermis, dermis, and subcutaneous tissue during (a) walking at $T_\infty = 15°C$, (b) walking at $T_\infty = 25°C$, and (c) walking at $T_\infty = 35°C$ and $E = 0\,\text{kg/m}^2\,\text{s}$.

where

$$I_1^{(e)} = \frac{1}{2}\iint_{\Omega^{(e)}} K^{(e)}\left[\left(\left(\frac{\partial T^{(e)}}{\partial x}\right)^2 + \left(\frac{\partial T^{(e)}}{\partial y}\right)^2\right)\right] d\Omega^{(e)}$$

$$I_2^{(e)} = \frac{1}{2}\iint_{\Omega^{(e)}}\left[\rho_b c_b w_b^{(e)}\left(T_A - T^{(e)}\right)^2\right] d\Omega^{(e)}$$

$$I_3^{(e)} = \frac{1}{2}\iint_{\Omega^{(e)}}\left[2\left(S_0 + \frac{E - S_0}{1 + e^{-}\beta(t - t_0)}\right)^{(e)} T^{(e)}\right] d\Omega^{(e)}$$

$$I_4^{(e)} = \frac{1}{2}\iint_{\Omega^{(e)}}\left[\rho c \frac{\partial T^{(e)2}}{\partial t}\right] d\Omega^{(e)}$$

$$I_5^{(e)} = \frac{1}{2}\int_{\Gamma_1^{(e)}}\left[h_{cr}\left(T^{(e)} - T_\infty\right)^2\right] d\Gamma_1^{(e)}$$

$$I_6^{(e)} = \frac{1}{2}\int_{\Gamma_1^{(e)}} LET^{(e)} d\Gamma_1^{(e)} \tag{24}$$

For the minimization of the function I, we have

$$\frac{\partial I}{\partial T_i} = \sum_{e=1}^{E}\frac{\partial I^{(e)}}{\partial T_i} = 0, \text{ for } i = 1, 2, \ldots, N. \tag{25}$$

Using equations (22) and (25), we get,

$$\frac{\partial I}{\partial T_i} = \sum_{e=1}^{E}\frac{\partial I^{(e)}}{\partial T_i} = \sum_{e=1}^{E}\frac{\partial}{\partial T_i}\left(I_1^{(e)} + I_2^{(e)} - I_3^{(e)} + I_4^{(e)} + I_5^{(e)} + I_6^{(e)}\right) = 0. \tag{26}$$

Differentiate equation (26) with respect to each nodal temperature T_0, T_1, and T_2 set the derivative equal to zero for the minimization. Equation (26) leads to a linear system of differential in the form

$$[Q]\{T\} + [A]\left\{\dot{T}\right\} = \{B\}. \tag{27}$$

The system of equation (27) can be solved by using the Crank–Nicolson method concerning time with the following relation

$$\left(A + \frac{\Delta t}{2}Q\right)T^{(i+1)} - \left(A - \frac{\Delta t}{2}Q\right)T^{(i)} = \Delta t B, \tag{28}$$

where Δt is the time interval and $T^{(i)}$ is the interface temperature of the epidermis, dermis, and subcutaneous tissue in the nth time step. On solving equation (28) repeatedly, we get the nodal temperature of each layer.

For the steady case of the model, we obtain the system of algebraic equations in matrix form as;

$$[Q]\{T\} = \{B\}. \tag{29}$$

5. Numerical Results

The threshold value of metabolic rate during walking is $3889.43\,\text{w/m}^3$, and during the marathon is $7918.00\,\text{w/m}^3$. The value of skin layers' thickness and physiological parameters used for numerical simulation has been taken as shown in Tables 1 and 2, respectively.

Assuming the ambient temperature is less than 37°C, the tissue temperature increases from the skin surface towards the body core. The increased tissue temperature $T(x, 0)$ shows in linear order given by the equation:

$$T(x, 0) = T_0 + \zeta x. \tag{30}$$

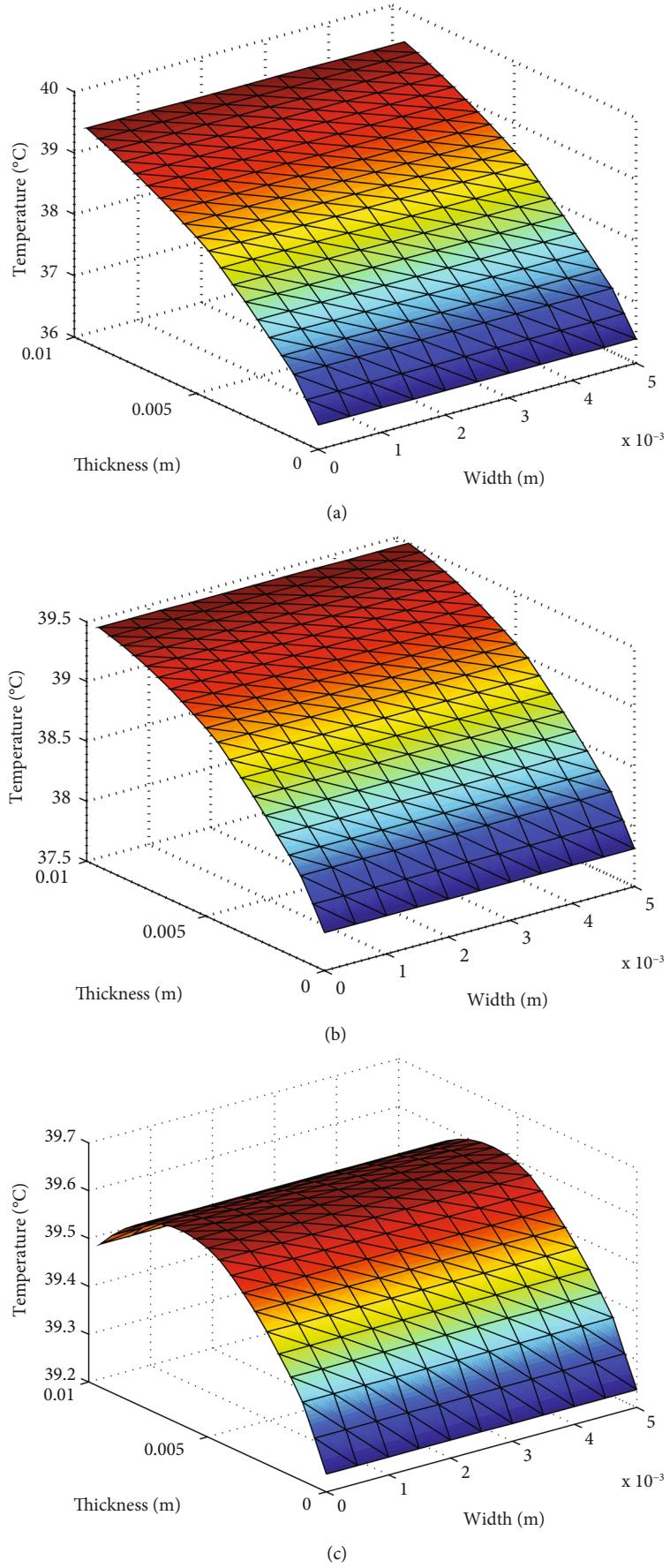

FIGURE 6: Estimation of steady state temperatures of the epidermis, dermis, and subcutaneous tissue during (a) marathon at $T_\infty = 15^\circ C$, (b) marathon at $T_\infty = 25^\circ C$, and (c) marathon at $T_\infty = 35^\circ C$ and $E = 0\,kg/m^2\,s$.

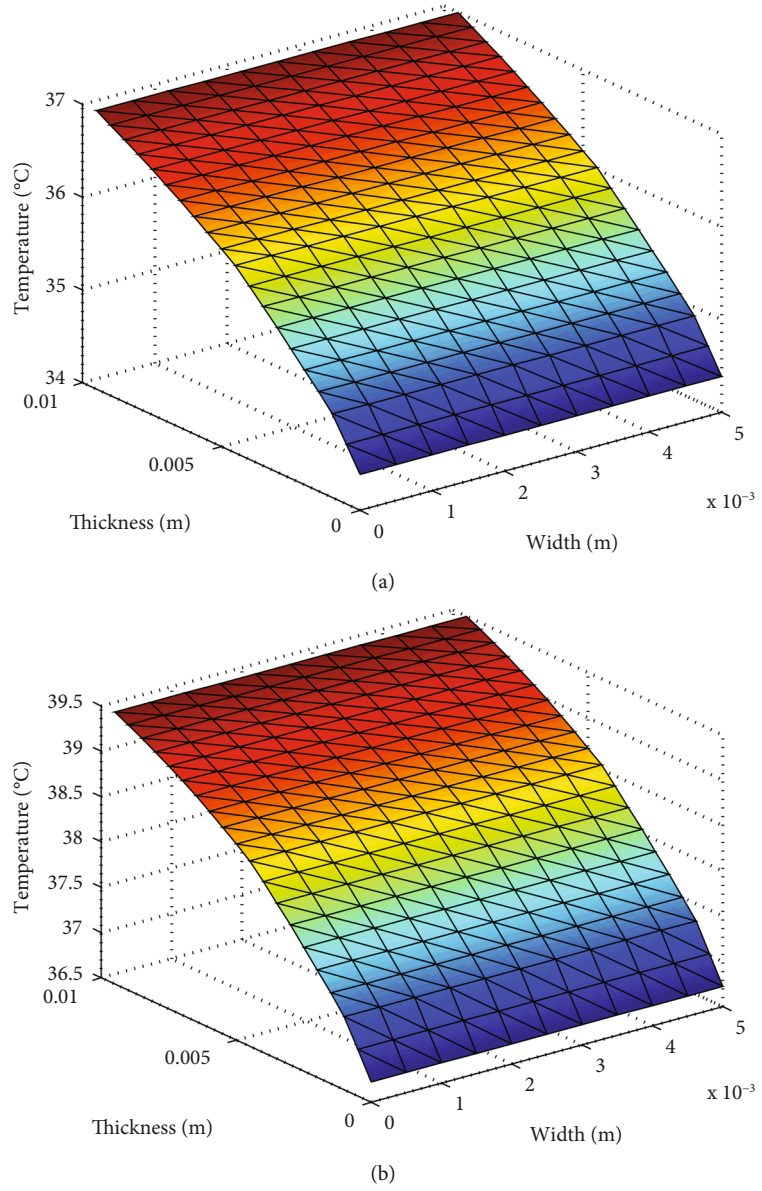

Figure 7: Comparison of steady-state temperatures $T^{(i)}$ $(i = 0, 1, 2)$ during (a) walking and (b) marathon at $T_\infty = 25^\circ\text{C}$ and $E = 0.00002\,\text{kg/m}^2\,\text{s}$.

The initial skin temperature is considered 24.91°C at normal ambient temperature. The use of ζ in equation (30) is constant, whose numerical value is determined by taking the known value $T_b = 37^\circ\text{C}$ for walking and $T_b = 39.5^\circ\text{C}$ for the marathon at $x = L_3$.

5.1. Steady State Temperature Results. The steady-state temperature results of the natural skin layers $T^{(i)}$, $(i = 0, 1, 2)$ for the epidermis, dermis, and subcutaneous tissue at the various ambient temperatures $T_\infty = 15^\circ\text{C}$, 25°C, and 35°C, and sweat evaporation rates $E = 0$, 0.00002, and $0.00004\,\text{kg/m}^2\,\text{s}$ during walking and marathon are calculated. The obtained results are presented through the graph in Figures 5, 6, 7, and 8 and Tables 3, 4, and 5.

On comparing the temperatures $T^{(i)}$ $(i = 0, 1, 2)$ between Figure 5 and Figure 6 during walking and marathon at $T_\infty = 15^\circ\text{C}$, 25°C, 35°C, and $E = 0\,\text{kg/m}^2\,\text{s}$, the skin layers temperature $T^{(0)}$, $T^{(1)}$, and $T^{(2)}$ have more by 2.38°C, 2.47°C, and 2.55°C, respectively, during the marathon compared with walking at each ambient temperature. These are due to more metabolic effects during the marathon. These results also have shown that the $T^{(2)}$ temperature reached 39.60°C at $T_\infty = 35^\circ\text{C}$ during the marathon without sweat evaporation. It may cause hyperthermia disorder. Therefore, the body controls the temperature by sensible perspiration process and keeps the body in thermoregulation.

Figure 7 shows the comparison of the skin layers' temperature $T^{(i)}$, $(i = 0, 1, 2)$ during walking and marathon at $T_\infty = 25^\circ\text{C}$ and $E = 0.00002\,\text{kg/m}^2\,\text{s}$. The graph of the results delineates that $T^{(0)}$ is more by 2.38°C, $T^{(1)}$ is more by 2.47°C, and $T^{(2)}$ is more by 2.55°C during the marathon compared

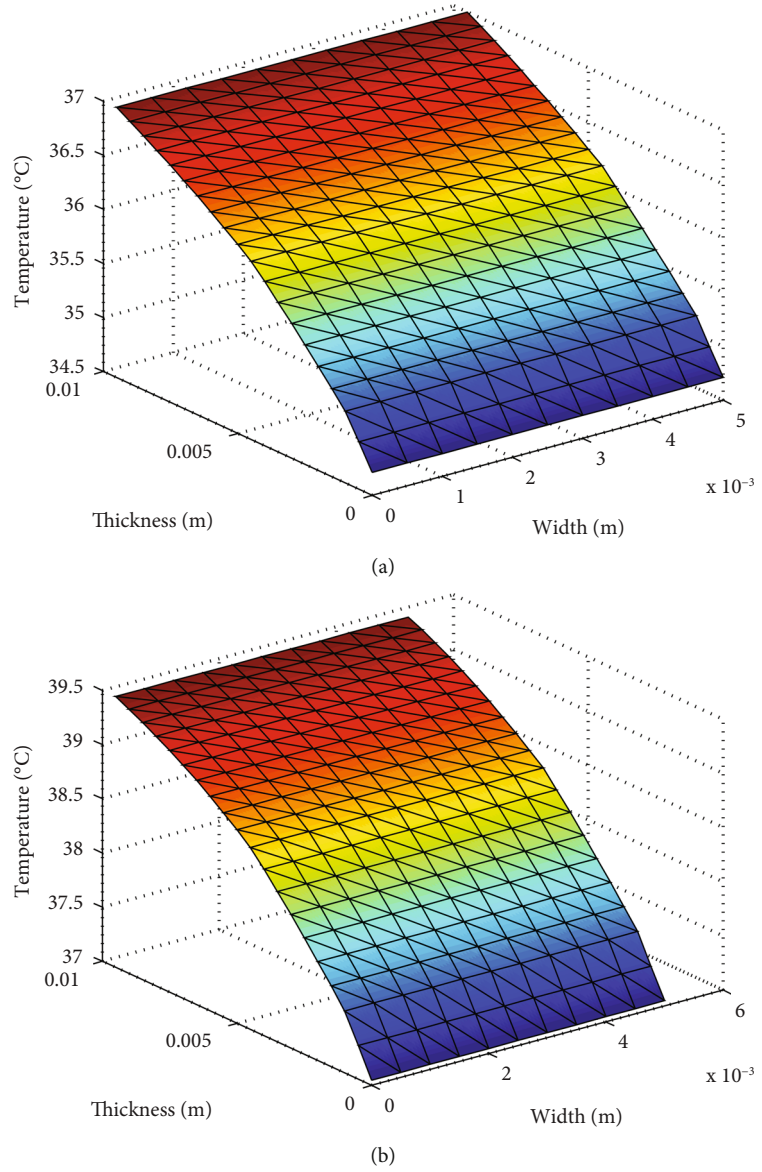

Figure 8: Comparison of steady-state temperatures $T^{(i)}$, $(i = 0, 1, 2)$ during (a) walking and (b) marathon at $T_\infty = 35^\circ\text{C}$ and $E = 0.00004\,\text{kg/m}^2\,\text{s}$.

Table 3: Estimation of steady state temperatures of the epidermis, dermis, and subcutaneous tissue during walking and marathon at $E = 0$ $\text{kg/m}^2\,\text{s}$.

Ambient Temperature (°C)	Skin layers temperatures during walking (°C)			Skin layers temperatures during marathon (°C)		
	Epidermis	Dermis	Subcutaneous	Epidermis	Dermis	Subcutaneous
15	34.34	35.19	36.47	36.72	37.66	39.02
25	35.63	36.10	36.76	38.01	38.57	39.31
35	36.92	37.01	37.05	39.30	39.48	39.60

with walking. These are due to more heat energy produced by the body during the marathon, and excess heat energy release helps to control the body temperature.

Figure 8 has presented the skin layers' temperature $T^{(i)}$, $(i = 0, 1, 2)$ during walking and marathon at $T_\infty = 35^\circ\text{C}$ and $E = 0.00004\,\text{kg/m}^2\,\text{s}$. These results reveal the temperatures $T^{(0)}$, $T^{(1)}$, and $T^{(2)}$ control to 34.93°C, 35.60°C, and 36.61°C during walking and 37.31°C, 38.08°C, and 39.15°C, by releasing sweat during the marathon, respectively. Due to high ambient temperature, the body gets energy from the hot environment

Table 4: Estimation of steady state temperatures of the epidermis, dermis, and subcutaneous tissue during walking and marathon at $E = 0.00002\,\text{kg/m}^2\,\text{s}$.

Ambient temperature (°C)	Skin layers temperatures during walking (°C)			Skin layers temperatures during marathon (°C)		
	Epidermis	Dermis	Subcutaneous	Epidermis	Dermis	Subcutaneous
15	33.35	34.49	36.25	35.73	36.96	38.80
25	34.64	35.40	36.54	37.02	37.87	39.09
35	35.93	36.31	36.83	38.30	38.77	39.37

Table 5: Estimation of steady state temperatures of the epidermis, dermis, and subcutaneous tissue during walking and marathon at $E = 0.00004\,\text{kg/m}^2\,\text{s}$.

Ambient temperature (°C)	Skin layers temperatures during walking (°C)			Skin layers temperatures during marathon (°C)		
	Epidermis	Dermis	Subcutaneous	Epidermis	Dermis	Subcutaneous
15	32.36	33.79	36.03	34.73	36.26	38.57
25	33.65	34.69	36.32	36.02	37.17	38.86
35	34.93	35.60	36.61	37.31	38.08	39.15

and increases the interface temperature. The study indicates that the temperature distribution has an enhancing effect on heat flux at the skin surface due to the exercises. On the other hand, the body plays a vital role, increasing the sweating rate has to reduce the temperature of the living tissues and keeps the body in thermoregulation during exercise.

5.2. Unsteady State Temperature Results. The unsteady state temperatures solution T_0 for the epidermis node, T_1 for the dermis node, and T_2 for the subcutaneous node are carried out by solving the system of equation (27). Figures 9, 10, 11, and 12 and Table 6 illustrate the unsteady state to steady state temperatures T_i, $(i = 0, 1, 2)$ during walking and marathon at $T_\infty = 15°\text{C}$, 25°C, and 35°C at various evaporation rates.

Figures 9 and 10 indicate the unsteady state temperatures, T_i at $E = 0.00002\,\text{kg/m}^2\,\text{s}$ in different ambient temperatures during walking and marathon. The results reveal that the temperature T_0 is more by 2.38°C, T_1 is more by 2.47°C, and T_2 is more by 2.55°C during the marathon compared with walking at $T_\infty = 15°\text{C}$. The temperatures, T_0, T_1, and T_2 is more by 2.37°C, 2.46°C, and 2.54°C, respectively, during a marathon compared with walking at $T_\infty = 35°\text{C}$. These are due to the body producing more metabolic heat energy during the marathon compared with walking. Figures 9 and 10 indicate that each temperature T_i, $(i = 0, 1, 2)$ increases on increasing the ambient temperatures from 15°C to 35°C, and T_2 shows the highest temperature at $T_\infty = 35°\text{C}$. Figures 9 and 10 also delineate that T_0 is less deviated and has reached faster in steady state from the unsteady state than T_1 and T_2 during both walking and marathon.

In comparing the unsteady state temperatures T_i, $(i = 0, 1, 2)$ during walking and marathon as presented in Figures 11(a) and 11(b). Figures 11(a) and 11(b) delineate that each nodal temperature has more during the marathon compared with walking. These are due to the more metabolic effect and conduct more heat energy during the marathon.

Figure 12 indicates the temperatures T_0 and T_2 during walking and marathon at $E = 0.00004\,\text{kg/m}^2\,\text{s}$ and $T_\infty = 35°\text{C}$. These results delineate that the temperatures, T_0 and T_2, rise higher and reach faster to the steady state during the marathon compared with walking. These are due to the faster movement of muscle mass during the marathon. The temperature T_2 is affected more due to the closer the subcutaneous tissue is to the body core.

5.3. Validity of the Temperature Results

5.3.1. Temperature during walking. Procter et al. studied the temperature occurring in the human body during moderate-intensity exercise. They suggested that the body core temperature occurs at $37 \pm 0.30°\text{C}$ during moderate-intensity exercise [28].

de Andrade Fernandes et al. suggested that the maximum body core temperature occurs at 37.70°C during moderate-intensity exercise. They indicated this experimental result in the published article [29].

Since the subcutaneous tissue is closer to the body's core, in our results, we observed that the maximum temperature of subcutaneous tissue during walking (moderate-intensity exercise) is 37.05°C. This result is closely equal to the body's core temperature during moderate-intensity exercise suggested by the researchers [28, 29]. Therefore, the temperature results obtained in this study during walking are valid.

5.3.2. Temperature During Marathon. Del Coso et al. suggested in their experimental study that during a 5-km marathon race, the body core temperatures rise rapidly at the beginning of the race and control the body core temperature up to 39.50°C [30].

Kenefick et al. suggested that the body core temperature in a human body occurs ranges from 38.50°C to 39.50°C during a marathon [2].

In this study, we obtained the maximum body core temperature during the marathon is 39.60°C. The result is nearly equal to the body core temperature suggested by the researchers

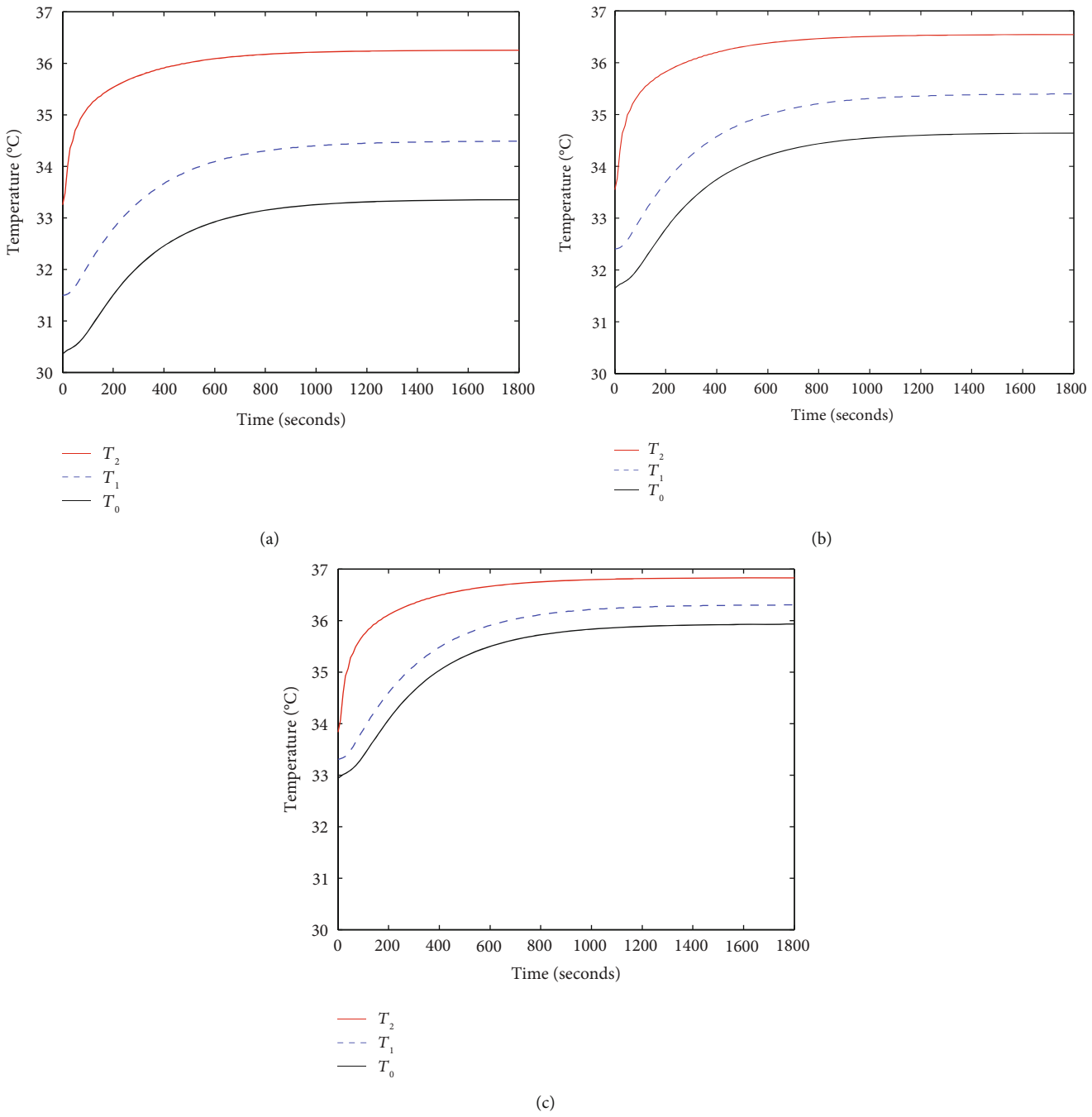

FIGURE 9: Observation of unsteady to steady state temperatures T_0, T_1, and T_2 during (a) walking at $T_\infty = 15^\circ$C, (b) walking at $T_\infty = 25^\circ$C, and (c) walking at $T_\infty = 35^\circ$C and $E = 0.00002\,\text{kg/m}^2\,\text{s}$.

during the marathon [2, 30]. Therefore, the temperature result conveyed in this study during the marathon is valid.

6. Stability and Convergence Analysis of the Solution

6.1. Stability Analysis. To show the stability of the solution of an equation in the two-dimensional discretization domain, it is sufficient to show the discretization is stable. For this, we use the following theorem.

6.1.1. Theorem. Let V_h be a continuous finite element space defined on the triangulation τ. f and b are the linear and bilinear forms of the problem $\|f\|_{L^2} < \infty$. Then finite element approximation T_h exists and discretization is stable in the H^1 norm.

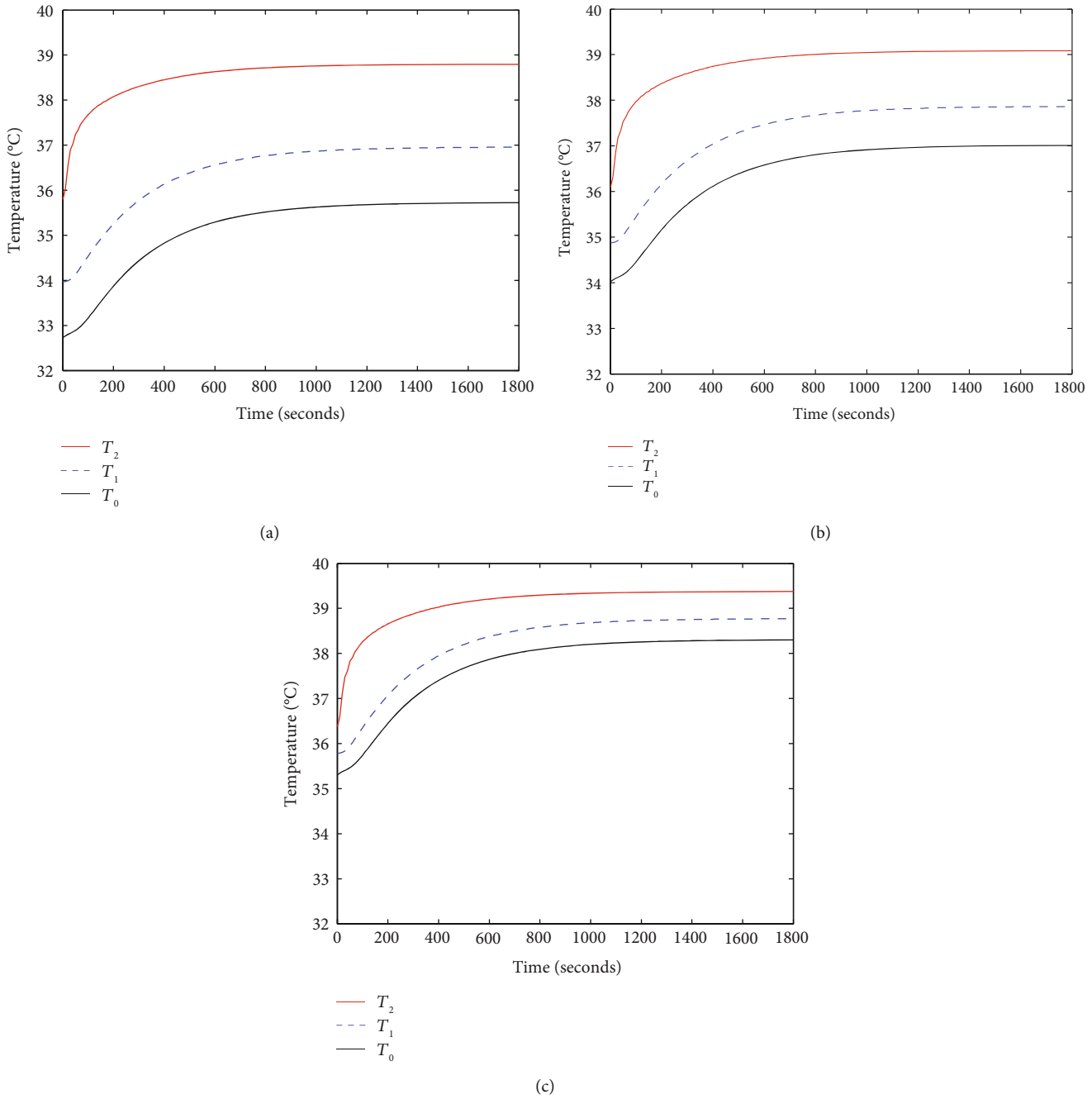

Figure 10: Observation of unsteady to steady state temperatures T_0, T_1, and T_2 during (a) marathon at $T_\infty = 15°C$, (b) marathon at $T_\infty = 25°C$, and (c) marathon at $T_\infty = 35°C$ and $E = 0.00002\,kg/m^2\,s$.

6.1.2. Proof. To prove the theorem, first, we have to show that F and b are continuous.

Where,

$$F = \int_\Omega f v \, dx$$
$$F \le \|f\|_{L^2} \|v\|_{L^2} \quad . \tag{31}$$

Since, $\|v\|_{H^1} \ge \|v\|_{L^2}$, so,

$$F \le \|f\|_{L^2} \|v\|_{H^1}$$

It shows that F is continuous.

$$\begin{aligned} |b(T, v)| &= |(T, v)_{H^1}| \\ &\le 1 \|T\|_{H^1} \|v\|_{H^1} \end{aligned} \quad . \tag{32}$$

Using Schwarz inequality of the inner product H^1, the bilinear form b is coercive.

$$|b(T, T)| = \left\|T^2\right\|_{H^1} \ge 1 \times \left\|T^2\right\|_{H^1}. \tag{33}$$

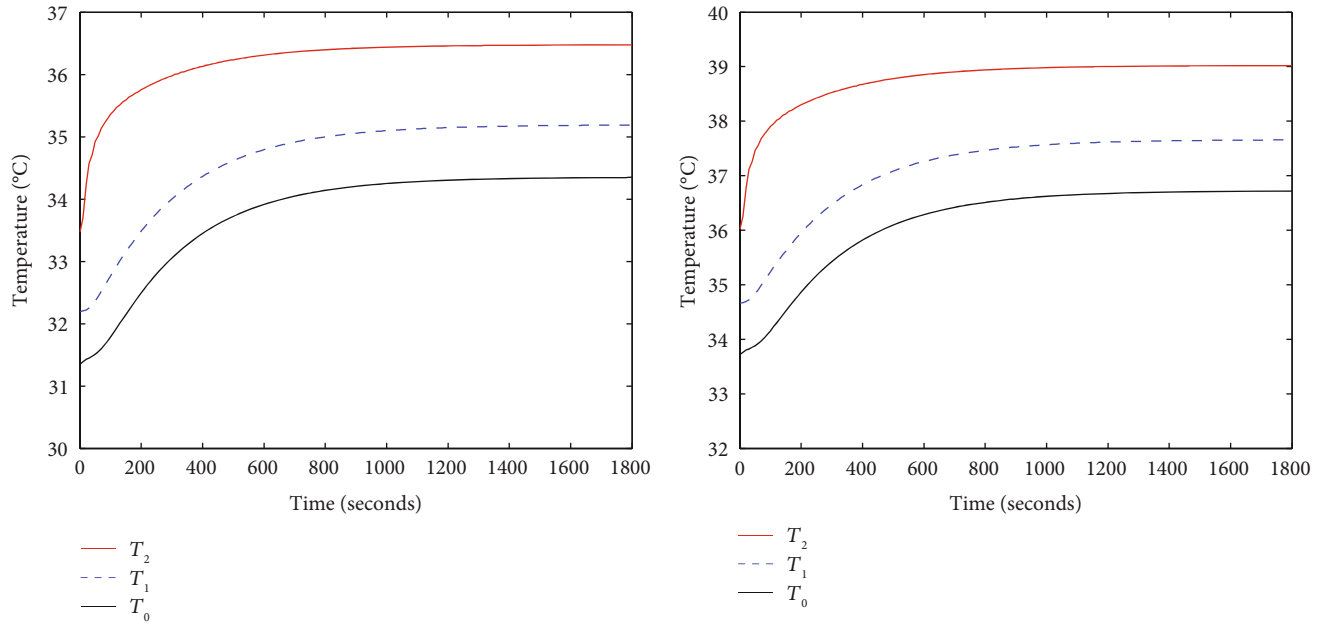

FIGURE 11: Comparison of T_0, T_1, and T_2 during (a) walking at $T_\infty = 15°C$ and (b) marathon at $T_\infty = 15°C$ and $E = 0\,\text{kg/m}^2\,\text{s}$.

Here, the continuity and coercivity constants both are 1, independent of space step size h, therefore, the discretization is stable.

6.2. Convergence of the Solution. Let T_h be the approximation solution with the exact solution T, of the problem. Then, for the convergence of the solution, it is sufficient to show that

$$\|T_h - T\|_{L^2}(\Omega) \le Ch^{k+1}\|T\|_{H^{k+1}}, \tag{34}$$

where k is the degree of Lagrange finite element approximation T_h. If m is the solution to the problem, then, Aubin–Nitsche duality argument provides

$$T - T_h = m - \nabla^2 m, \tag{35}$$

where m has the same Neumann condition as T.

Since $T - T_h \in H^1(\Omega) \subset L^2(\Omega)$the elliptic regularity provides that $m \in H^2(\Omega)$

Then, using the testing function v and integrating by parts we get,

$$b(m, v) = (T - T_h, v)_{L^2(\Omega)} \forall v \in H^1(\Omega), \tag{36}$$

and so

$$\begin{aligned} \|T - T_h\|^2_{L^2(\Omega)} &= (T - T_h, T - T_h) \\ &= b(m, T - T_h) \\ &= b(m - I_h m, T - T_h) \quad \text{using orthogonality} \end{aligned} \tag{37}$$

I_h denotes the global interpolating mapping with $\|m - I_h m\|_{H^1(\Omega)} \le C^* h^{k+1}|T|_{H^{k+1}(\Omega)}$

$$\begin{aligned} \text{Now, } \|T - T_h\|^2_{L^2(\Omega)} &\le C\|I_h m - m\|_{H^1(\Omega)}\|T - T_h\|_{H^1(\Omega)} \\ &\le CC^* h^{k+1}\|T - T_h\|_{L^2(\Omega)}|T|_{H^{k+1}(\Omega)} \end{aligned} \tag{38}$$

dividing both sides by $\|T - T_h\|_{L^2(\Omega)}$ we get

$$\|T - T_h\|_{L^2(\Omega)} \le CC^* h^{k+1}|T|_{H^{k+1}(\Omega)}, \tag{39}$$

gives the result. Thus, the solution is convergent with space step size h by using the L^2 norm instead of the H^1 norm.

7. Conclusion

The results in the model analyze that the steady temperature of skin layers $T^{(i)}$, $(i = 0, 1, 2)$ is higher during the marathon than walking due to more metabolic effects. These results indicate that the temperature of the human body increases by increasing the activity level. However, due to the threshold value of body core temperature, the body loses more heat energy during the marathon compared with walking in the form of sweat and frequently controls the body temperature. It indicates that the sweating mechanism plays a vital role in protecting the body from hyperthermia sickness during walking and the marathon.

Earlier researchers developed many mathematical models in the temperature distribution in the human dermal parts, but they have not determined the metabolic rate during the exercise period. Therefore, this model is prepared for the

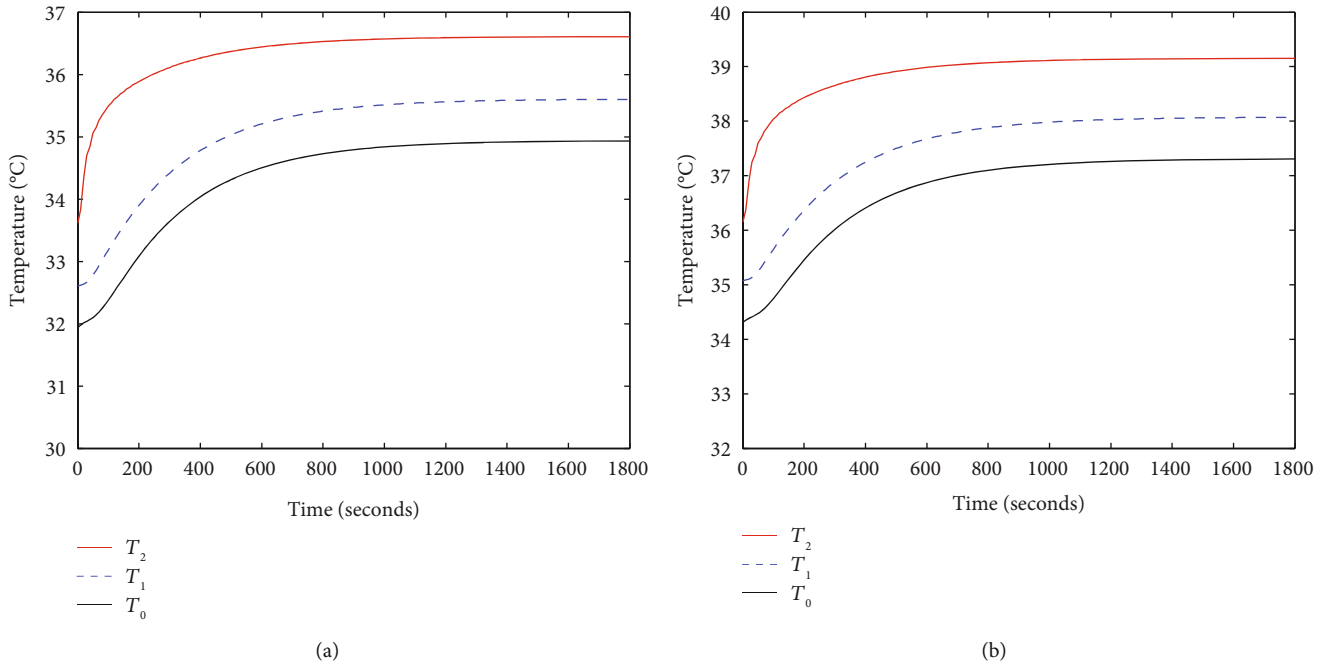

Figure 12: Comparison of T_0 and T_2 during (a) walking $T_\infty = 35°C$ and (b) marathon at $T_\infty = 35°C$ and $E = 0.00004\,kg/m^2\,s$.

Table 6: Estimation of unsteady state to steady state nodal temperature T_0, T_1, and T_2 during walking and marathon at $E = 0.00004\,kg/m^2\,s$.

Ambient temperature (°C)	Skin nodal temperatures during walking (°C)			Skin nodal temperatures during marathon (°C)		
	T_0	T_1	T_2	T_0	T_1	T_2
15	32.36	33.79	36.03	34.73	36.26	38.57
25	33.65	34.69	36.32	36.02	37.17	38.86
35	34.93	35.60	36.61	37.31	38.07	39.15

realistic temperature distribution in dermal parts of the human body with the metabolic rate during walking and marathon. The various sweat evaporation rates and ambient temperatures have been used in this model. Therefore, this research study will assist to maintains the physical structure of aging and pregnant women. It also uses to develop the model regarding the different exercises as a sports player, mountain climber, laborer, plumber, typist, and driver based on their physical and physiological parameters.

Data Availability

Data supporting this research article are available from the corresponding author or First author upon reasonable request.

Conflicts of Interest

The author(s) declare(s) that they have no conflicts of interest.

References

[1] T. Gasparetto and C. Nesseler, "Diverse effects of thermal conditions on performance of marathon runners," *Frontiers in Psychology*, vol. 11, p. 1438, 2020.

[2] R. W. Kenefick, S. N. Cheuvront, and M. N. Sawka, "Thermoregulatory function during the marathon sports," *Sports Medicine*, vol. 37, no. 4–5, pp. 312–315, 2007.

[3] M. H. Malekmohamadi, H. Ahmadikia, and M. Mosharaf-Dehkordi, "The effect of heat flux distribution and internal heat generation on the thermal damage in multi-layer tissue in thermotherapy," *Journal of Thermal Biology*, vol. 99, no. 1, pp. 1–11, 2021.

[4] B. M. Marriott, *Nutritional Needs in Hot Environments: Applications for Military Personnel in Field Operation*, pp. 1–392, National Academies Press, Washington, DC, 1993, https://www.ncbi.nlm.nih.gov/books/NBK236225/.

[5] L. G. Pugh, J. L. Corbett, and R. H. Johnson, "Rectal temperatures, weight losses, and sweat rates in marathon running," *Journal of Applied Physiology*, vol. 23, pp. 347–352, 1976.

[6] B. Sperlich, *Marathon Running: Physiology, Psychology, Nutrition and Training Aspects*, pp. 1–12, Department of Sport Science Julius-Maximilians-Universität Würzburg, Bayern, Germany, 2016.

[7] J. D. Hardy, "The radiation of heat from the human body: III. The human skin as a black body radiator," *The Journal of Clinical Investigation*, vol. 13, no. 4, pp. 615–620, 1934.

[8] A. E. Tansey and D. C. Jonson, "Recent advances in thermoregulation," *Advances in Physiology Education*, vol. 39, pp. 139–148, 2015.

[9] A. Bera, S. Duttaa, J. C. Misrab, and G. C. Shit, "Computational modeling of the effect of blood flow and dual phase lag on tissue temperature during tumor treatment by magnetic hyperthermia," *Mathematics and Computers in Simulation*, vol. 188, pp. 389–403, 2021.

[10] P. A. Bradbury, R. H. Fox, R. Goldsmith, and I. F. G. Hampton, "The effect of exercise on temperature regulation," *The Journal of Physiology*, vol. 171, pp. 384–396, 1964.

[11] G. C. Shit and A. Bera, "Mathematical model to verify the role of magnetic field on blood flow and its impact on thermal behavior of biological tyissue for tumor treatment," *Biomedical Physics and Engineering Express*, vol. 6, article 015032, 2020.

[12] M. Kleiberi, "Body size and metabolism," *Hilgardia*, vol. 6, pp. 315–353, 1932.

[13] S. Acharya, *Mathematical Study of Temperature Distribution Model in Human Males and Females Dermal Part*, pp. 1–173, Kathmandu University, Nepal, 2015, PhD Thesis.

[14] D. C. Shrestha, S. Acharya, and D. B. Gurung, "Modeling on metabolic rate and thermoregulation in three layered human skin during carpentering, swimming and marathon," *Applied Mathematics*, vol. 11, pp. 753–770, 2020.

[15] D. C. Shrestha, S. Achayra, and D. B. Gurung, "A finite element approach to evaluate the thermoregulation in human body due to the effects of sweating during walking, cleaning, and cooking," *Mathematical Problems in Engineering*, vol. 2021, 2021.

[16] I. D. Stephen, V. Coetzee, M. L. Smith, and D. I. Perrett, "Skin blood perfusion and oxygenation colour affect perceived human health," *PLoS One*, vol. 4, no. 4, article e5083, 2009.

[17] G. C. Shit and A. Bera, "Temperature response in a living tissue with different heating source at the skin surface under relaxation time," *International Journal of Applied and Computational Mathematics*, vol. 3, pp. 381–394, 2015.

[18] H. H. Pennes', "Analysis of tissue and arterial blood temperature in resting human forearm," *Journal of Applied Physiology*, vol. 1, no. 2, pp. 93–122, 1948.

[19] S. M. Day and P. D. Thompson, "Cardiac risks associated with marathon running," *Sports Health*, vol. 2, no. 4, pp. 301–306, 2010.

[20] K. C. Gokul, D. B. Gurung, and P. R. Adhikary, "Effect of blood perfusion and metabolism in temperature distribution in human eye," *Advances in Applied Mathematical Biosciences*, vol. 4, no. 1, pp. 13–23, 2013.

[21] S. Acharya, D. B. Gurung, and V. P. Saxena, "Two dimensional finite element method for metabolic effect in thermoregulation on human males and females skin layers," *Journal of Coastal Life Medicine*, vol. 3, no. 8, pp. 623–629, 2015.

[22] M. Agrawal, K. R. Pardarsani, and N. Adlaka, "State temperature distribution in dermal regions of an irregular tapered shaped human limb with variable eccentricity," *Journal of Thermal Biology*, vol. 44, pp. 27–34, 2014.

[23] D. B. Gurung, "Two dimensional temperature distribution model in human dermal region exposed at low ambient temperature with airflow," *Kathmandu University Journal of Science, Engineering and Technology*, vol. 8, no. 2, pp. 11–24, 2012.

[24] M. A. Khanday and V. P. Saxena, "Finite element approach for the study of thermoregulation in human head exposed to cold environment," *Proceedings of American Institute of Physics*, vol. 1146, pp. 375–385, 2009.

[25] B. Partovi, H. Ahmadikia, and M. M. Dehkordi, "Analytical and numerical temperature distribution in a 3-D triple layer skin tissue subjected to a multi-point laser beam," *Journal of Engineering Mathematics*, vol. 131, no. 13, pp. 1–14, 2021.

[26] P. Seshu, *Textbook of Finite Element Analysis*, pp. 1–327, PHI Learning Private Limited, New Delhi, India, 2012.

[27] D. B. Gurung, V. P. Saxena, and P. R. Adhikari, "FEM approach to one dimensional unsteady state temperature distribution in human dermal parts with quadratic shape function," *Journal of Applied Mathematics and Informatics*, vol. 27, no. 1–2, pp. 301–313, 2009.

[28] E. Procter, G. Strapazzon, H. Gatterer, and B. Wallner, "Monitoring body temperature during moderate-intensity exercise and inactive recovery in the cold: a pilot study," *Current Issues in Sport Science*, vol. 3, p. 14, 2018.

[29] A. de Andrade Fernandes, P. R. dos Santos Amorim, and C. J. Brito, "Regional skin temperature response to moderate aerobic exercise measured by infrared thermography," *Asian Journal of Sports Medicine*, vol. 7, no. 1, p. e29243, 2016, 1.

[30] J. Del Coso, D. Fernandez, and J. Abian-Vicen, "Running pace decrease during a marathon is positively related to blood markers of muscle damage," *PLoS One*, vol. 8, no. 2, article e57602, 2013.